Appl. Phys. A (2016) 122:368
DOI 10.1007/s00339-016-9880-6

Applied Physics A
Materials Science & Processing

Subwavelength grating waveguides for integrated photonics

Hamdam Nikkhah[1] · **Trevor J. Hall**[1]

Received: 16 August 2015 / Accepted: 17 November 2015 / Published online: 14 March 2016

Abstract Subwavelength waveguide gratings (SWG) are locally periodic structures with parameters that may vary slowly on the scale of a wavelength. Here the implementation of a Lüneburg lens as a SWG to provide Fourier optics on a chip and the design of the adiabatic structures that must be provided to interface SWG structures to conventional waveguides are considered. Preliminary findings are reported on the dispersion engineering of multimode interference couples towards the ideal port phase relations needed in coherent applications.

1 Introduction

There is considerable interest in the field of optical communications in the integration of devices using a silicon-based materials platform to decrease component footprint and cost. Immense advances have been made, all the basic functions needed having been demonstrated. Nevertheless, there remain technical and economic roadblocks to widespread adoption of the technology. A fundamental difficulty is that silicon is not suitable for light emission or, to a lesser extent, modulation. Si photonics has therefore been primarily restricted to the integration of passive functions. Active functions are provided by discrete devices such as off-chip lasers based on InP and separately packaged $LiNb0_3$ modulator circuits. Even then there remains a formidable challenge to the efficient transfer of light energy between the different waveguide technologies that must be interfaced.

Rapid and continuous progress in nanofabrication means that electromagnetic materials can now be engineered at a subwavelength scale. A recent breakthrough is to use subwavelength structures to tailor the refractive index and dispersion properties of integrated components. This has been applied with great success in a wide variety of applications of silicon photonics to radically reduce coupling loss, excess insertion loss and crosstalk and to dramatically increase the operational bandwidth of components [1].

Fortunately, it is now practical to engineer the optical properties of structures on a chip by subwavelength patterning in a single etch step of binary nanocomposite material with a feature size that is not limited to expensive high-resolution techniques such as electron-beam lithography. This offers fabrication processes amenable to the economics of mass manufacture.

Our work focuses on subwavelength waveguide gratings (SWG) that are periodic on the scale of a subwavelength lattice with parameters that vary on a scale larger than a wavelength. In Sect. 2, the SWG structure, the design and verification challenges and the principles of homogenisation are discussed. In Sect. 3 results of simulations of graded SWG structures are presented and a Mach–Zehnder interferometer structure for the measurement of the effective refractive index of SWG is introduced. Section 4 provides a brief discussion on the use of SWG to control spatial dispersion in the context of approaching an ideal multimode interference couplers, and Sect. 5 draws some conclusions.

✉ Hamdam Nikkhah
hnikk057@uottawa.ca

[1] Photonics Technology Laboratory, Centre for Research in Photonics, School of Electrical Engineering and Computer Science, University of Ottawa, Advanced Research Complex, 25 Templeton St., Ottawa, ON K1N 6N5, Canada

2 Homogenisation

In photonic crystal structures a waveguide is typically created by introducing a line defect. At an operating frequency within the bandgap, guiding may occur due to the mirror-like effect of the lattice surrounding the defect. At an operating frequency outside the bandgap, guiding may occur when the effective index of the lattice is lowered from that of the line defect (e.g. by hole inclusions). Subwavelength waveguide gratings are a subcategory of photonic crystal structure that operate at frequencies below the bandgap and require no surrounding lattice to guide. The fundamental wave-guiding principle is the propagation of the Floquet–Bloch modes of the SWG. Silicon SWG crossings and photonic wires have been demonstrated that have experimentally measured losses of -0.07 dB per crossing and 3.1 dB cm^{-1}, respectively [2], which is astonishing given that the light passes through 60,000 interfaces every centimetre.

The combination of subwavelength scale nanostructures with overall component dimensions measured in hundreds of wavelengths creates computational problems of massive scale as the current tools require computational meshes that are sufficiently fine to adequately sample the nanostructure. Available tools rapidly run out of resources, or produce results that cannot be trusted. The absence of a reliable means to model and simulate large-scale nanostructures is a major roadblock to advances in nanophotonics. Current tools for component simulation require subwavelength computational meshes that can only be applied to nanostructured regions a few wavelengths in extent. Modelling at larger scales requires an abstraction of the properties of the nanostructure, which summarises its properties pertinent to the larger scale and smooths over the detail at the smaller scale. This abstraction is known as homogenisation. Investigation of the behaviour of the mode and effective mode index with respect to fill factor of the patterned structure outside parameter regions where simple effective material theory applies is the motivation for the study reported in this paper.

There is a vast literature on homogenisation. Its classic roots are the Clausius–Mossotti equation [3] that links the electrodynamics of continuous media to their atomic structure and the mixture formulae of Maxwell Garnet [4] for the constitutive parameters of composite materials. Early studies applied long-wavelength asymptotic approximations because all but simple problems, such as the 1D lamellar structure analysed by Rytov [5], are intractable theoretically. A resurgence of interest in homogenisation can be traced to Prof. Sir John Pendry's corpus of work on negative refractive index materials, first postulated by Veselago [6]; and to an influential paper by Smith and Pendry [7] in which they pointed out that the electromagnetic fields in a unit cell of a photonic crystal may be calculated advantageously by commercial tools; albeit, there remains additional coding to complete the homogenisation. The method of Smith and Pendry has been shown to be flawed in certain circumstances [8], but that of Pérez-Huerta et al. [9], which draws on early work by Mochán and Barrera [10], and Mochán et al. [11] is compelling.

In the case of periodic dielectric structures, one may use a (commercially available) band solver to find the homogenised parameters for internal Bloch modes that describe light well away from the surface of a finite-sized photonic crystal where the translation symmetry is broken. The Bloch mode expansion must be completed by evanescent Bloch modes, i.e. modes with a complex Bloch wave vector, which represent waves bound to the surface [12].

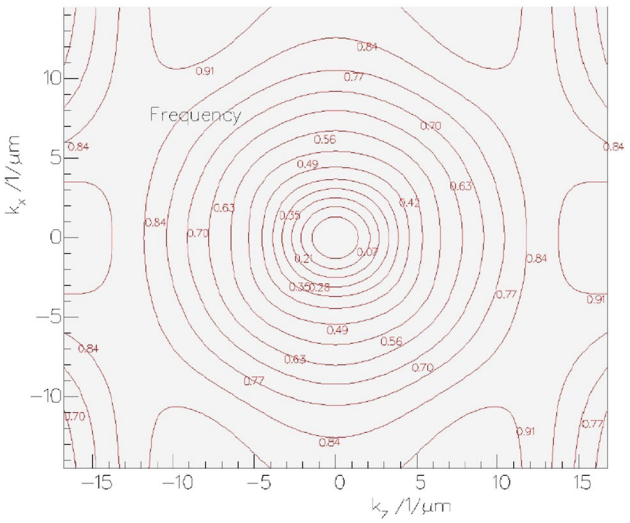

Fig. 1 Equi-frequency contours of the band surface displayed on the wave vector plane

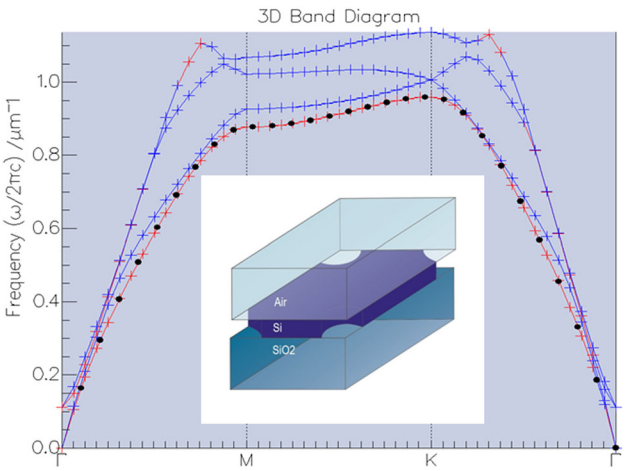

Fig. 2 3D unit cell analysis and the band diagram

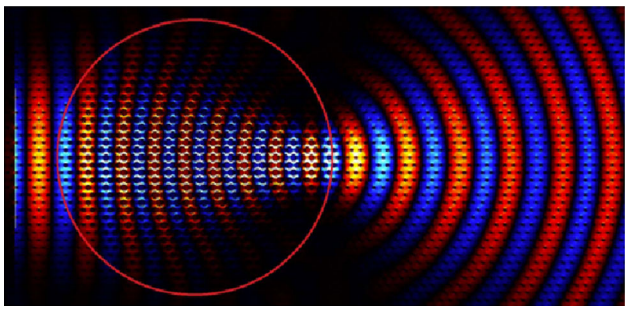

Fig. 3 A FDTD simulation of an incident plane wave focused by a planar graded metamaterial lens. The local structure of the Bloch wave as a product of a periodic function with the same period as the lattice and a Bloch phase factor describing the phase advance across unit cells is clearly visible

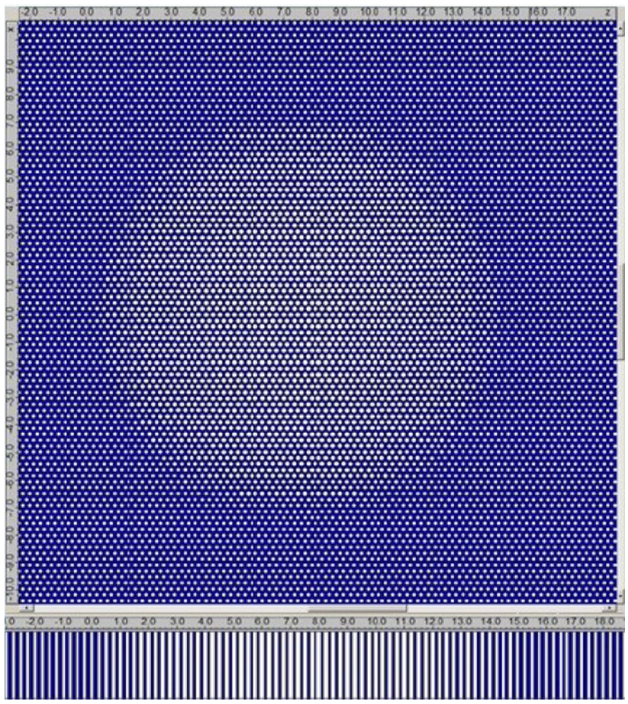

Fig. 4 A metamaterial Lüneburg lens with a diameter of 15 μm; with the rod diameters varying from 151 nm on the rim to 202 nm in the centre placed on a hexagonal lattice with lattice constant of 250 nm. The effective refractive index on the rim was set to 1.4, which leads to an effective index at the centre of the lens of 1.98. The calibration used was appropriate to 2D FDTD simulation

Commercial band solvers assume a material of infinite extent; consequently, resort must be made to general purpose finite element method (FEM) or finite-difference time-domain (FDTD) solvers with additional programming effort. For a slab, one must match a Rayleigh plane wave expansion in the exterior domain to a Bloch plane wave expansion in the interior domain. The transverse component of the exterior plane wave and internal Bloch wave vector must match by field continuity considerations. This justifies the use of the effective index of the Bloch mode as the homogenised index. It also suggests that the correct method of smoothing the field is to set the amplitude of spatial frequencies outside the first Brillouin zone to zero. A plane wave expansion approach similar to that used in band solvers can then be used to solve for the averaged fields to find material constitutive parameters. The result is essentially exact: the full band structure accessible by an exterior wave may also be reconstructed from the homogenised parameters.

Graded structures may be described by introducing two spatial scales: a ‘slow’ base-space coordinate pertinent to the variation of the nanostructure parameters (e.g. atom size, lattice ‘constant’) and a ‘fast’ tangent space coordinate pertinent to a periodic extension of the local nanostructure. The hope is that the structure in the neighbourhood of the base-space position is well approximated by the periodic extension of the nanostructure at that position. This is an asymptotic approximation that we have applied with success in numerical experiments on the metamaterial Lüneburg lens [13]. A similar approach to grading but relying on the less precise Maxwell–Garnett effective index formulae is described in [14].

3 Simulation results

An interest in Fourier optics on a chip [13] provided our starting point: the implementation of a planar Lüneburg lens as a slowly varying photonic crystal slab waveguide (or ‘metamaterial’). A hexagonal lattice was chosen as this offered a band structure with circular equi-frequency contours in the long-wavelength operational limit, shown in Fig. 1.

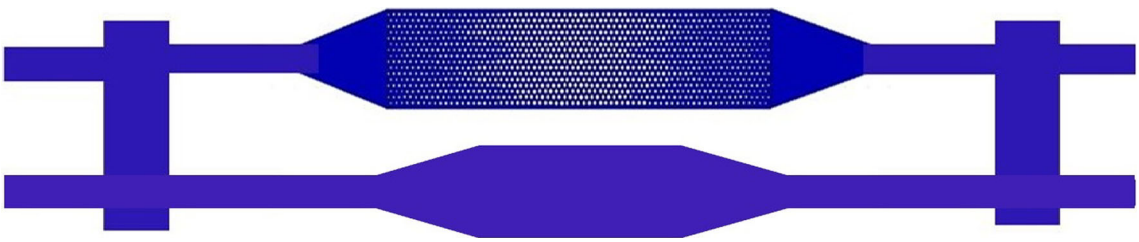

Fig. 5 MZI structure with one arm patterned structure and the other arm silicon

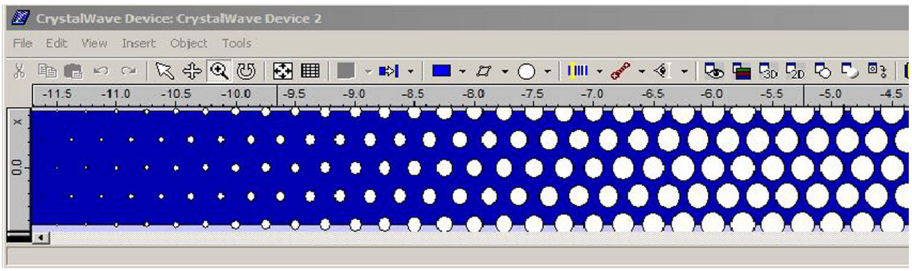

Fig. 6 An enlargement of the upper arm of the MZI showing detail of the homogenised refractive index taper

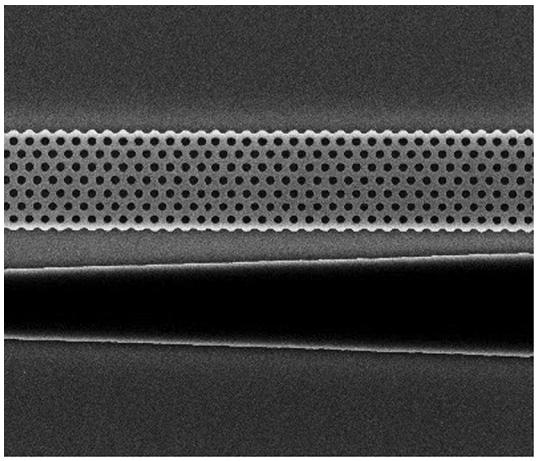

Fig. 7 SEM of two arms of MZI at the central section, holes with constant diameters

The local index was found by two methods. In the first method, a band solver was used to predict the homogenised index of a Bloch mode in a two-dimensional photonic crystal of infinite extent. This homogenised index was then used as the core index in an orthodox model of an asymmetric slab waveguide to predict the effective index of the mode bound to the slab.

In the second approach, a 3D unit cell is defined by periodically replicating, in the direction normal to the plane, the waveguide structure containing a single 2D unit cell in the plane. The out-of-plane period is chosen large enough that the waveguide fields are negligible at the upper and lower end faces of the unit cell. A 3D band solver is then used to directly determine the effective index of the fundamental mode of the patterned slab waveguide structure. A representative 3D unit cell is shown in Fig. 2, consisting of three layers of air, metamaterial and silica.

The assumption of an infinite number of replications of the 3D unit cell normal to the plan of the slab is an approximation given that the slab is only one unit cell thick, which causes a small error in the field due to the periodicity assumption. Hence, the 3D band structure solver for a 2D periodic medium can give an accurate value of the effective index of the metamaterial, but is computationally more demanding.

Remarkably, the two methods agree very closely [13]. This indicates first that the evanescent fields generated at the upper and lower boundaries of the core do not significantly tunnel across the core despite its small thickness of 300 nm and second that the field continuity conditions at the core boundaries differ little from that for continuous media despite the patterning of the core.

To fully exploit the flexibility offered by subwavelength grating structures they need to be integrated and interconnected by conventional waveguides. In the case of the Lüneburg lens, it is fortunate that the structure naturally features an adiabatic transition from the exterior domain at the rim to the interior structure of the lens [13]. The lens can be made in two ways: using either air holes in silicon layer or silicon rods in air. Figure 3 shows an example of subwavelength structure implementation of a planar Lüneburg lens, using air holes in the silicon layer. Figure 4

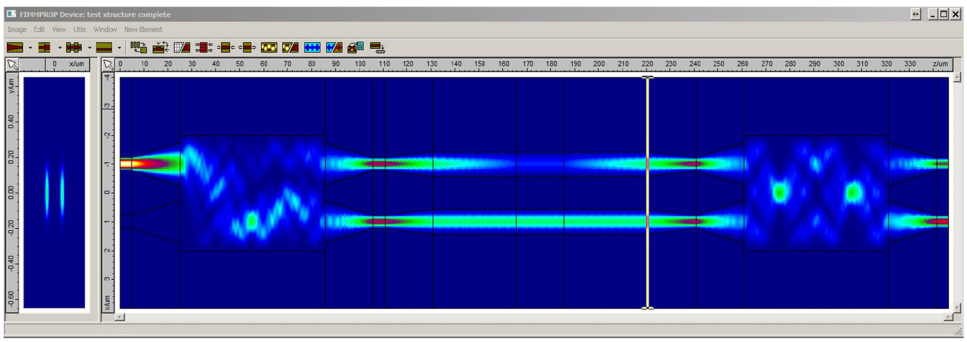

Fig. 8 FimmProp simulation of a MZI structure with upper arm containing homogenised SWG waveguide and the lower arm containing standard silicon waveguides

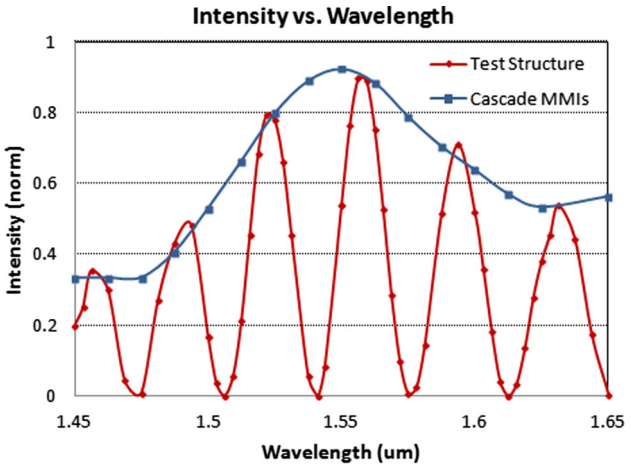

Fig. 9 MZI output intensity against wavelength for a SWG test structure of the length 20 μm (*red*) illustrating the spectral fringes due to the optical path imbalance introduced by the SWG section. Also shown is the output intensity of an empty MZI (back-to-back MMIs) (*blue*) which follows the envelope of the spectral fringes

shows the metamaterial lens structure using silicon rods in air. The structure of air holes in the silicon layer is preferred in this study because it offers a wider range of homogenised index compared to silicon rods in air.

In general, however, it is necessary to provide adiabatic structures that not only adapt waveguide dimensions but also adapt the homogenised index. Figure 5 shows an example of a Mach–Zehnder interferometer with a length of subwavelength grating waveguides within their arms adapted to standard silicon waveguides by adiabatic tapers. The SWG is interfaced to standard silicon waveguides first by an adiabatic taper with varying width and constant refractive index and then by an adiabatic taper of constant width but varying homogenised index. The lower arm contains standard silicon waveguide identical in the length with the upper arm, and includes the geometrical tapers and a solid central section. The homogenized index tapers are omitted. The imbalance between the arms will allow the experimental measurement of the homogenised index.

Figure 6 shows an enlargement of the arm showing the detail of the homogenised refractive index taper, while the diameter of the air holes is increasing from left to right. Figure 7 shows the first SEM released of the two arms of MZI at the central section where the diameter of holes is constant.

These structures are an example of a case where a nanoscale simulation over the full device, say using FDTD, is not reliable. Rather, we have relied on simulation of the homogenised structures using FimmProp as shown in Fig. 8, together with the calibration procedure described for the Lüneburg lens.

The experimental confirmation of the validity or otherwise of the calibration approach awaits the Lüneburg lens and MZI structures to come out of fabrication.

Figure 9 shows the intensity at the output port of the MZI with wavelength scanned from 1.45 to 1.65 μm for a SWG test structure (shown in Fig. 8) of length 20 μm (red) which illustrates the spectral fringes due to the optical path length imbalance introduced by the test section. These fringes provide a measurement of the homogenised refractive index. Also shown is the output intensity of an empty MZI (back-to-back MMIs, shown in Fig. 10) (blue) which follows the envelope of the spectral fringes.

4 Discussion

Now that coherent transmission is so well entrenched, extra care is required to control the phase in addition to the amplitude of light propagating in photonic integrated circuits. The phase relationship between the ports of splitters and couplers is particularly important in applications to microwave frequency multiplication, advanced I–Q modulation, optical hybrids for coherent receivers and more

Fig. 10 Back-to-back MMIs to obtain the envelope of the spectral fringes

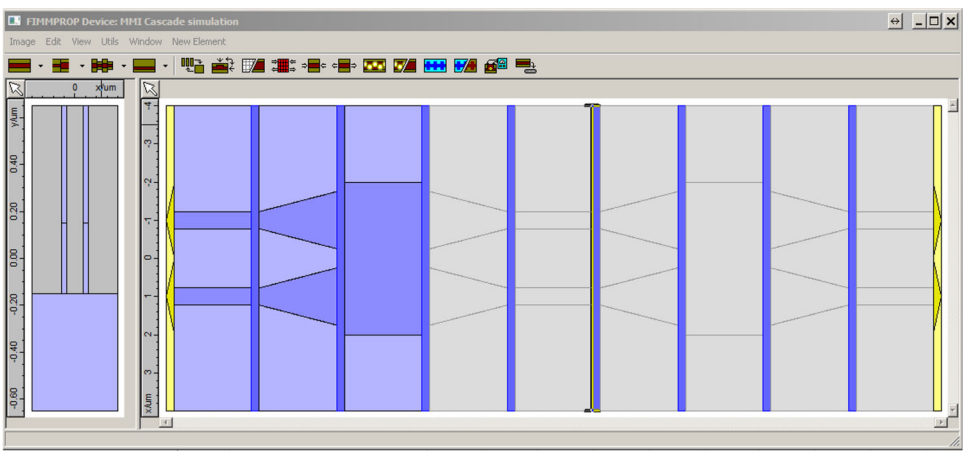

[15–20]. In particular, this leads to the search for a perfect multimode interference (MMI) coupler in which subwavelength waveguide gratings are used to engineer the dispersion and anisotropy of the MMI so that a practical device provides close to the ideal (but normally approximate) self-imaging behaviour. To this end, a slab waveguide patterned as a photonic crystal in one dimension is being investigated. Very good agreement between the band solver and the Kronig–Penney model has been obtained for Bloch vectors in the plane of the slab and not just normal to the grating structure. There is, however, a substantial difference between the mapping of the homogenised index to the mode effective index via the asymmetric slab waveguide model and the predictions of the band solver for a 3D unit cell. Whether this is because of the difficulties in ensuring that a commercial band solver finds the correct band structure for this geometry or the assumptions inherent in the indirect approach remain valid is the subject of further investigation.

5 Conclusions

The continuing improvement in advanced lithography techniques (such as immersion lithography, extreme-UV lithography, nanostepping lithography) will enable accurate, large-volume production of subwavelength structures and devices. The use of SWG structures in integrated photonics devices is thus likely to continue to expand, enabling new functionalities and devices to be designed and fabricated, and these SWG structures will become an essential tool set in advanced photonic design libraries.

Acknowledgments The authors are indebted to Tom Davies of Technix for his technical support of the Photon Design suite of software tools used in the work. The authors acknowledge the financial support of the Natural Sciences and Engineering Research Council of Canada (NSERC) though an Engage Grant with Technix. Trevor J. Hall is grateful to the Canada Research Chair (CRC) Program for their support of his CRC-I in Photonic Network Technology.

References

1. R. Halir et al., Waveguide sub-wavelength structures: a review of principles and applications. Laser Photon. Rev. **9**(1), 25–49 (2015)
2. P.J. Bock, P. Cheben, J.H. Schmid, J. Lapointe, A. Delage, D.X. Xu, S. Janz, A. Densmore, T.J. Hall, Subwavelength grating crossings for silicon wire waveguides. Opt. Express **18**(15), 16146–16155 (2010)
3. J.H. Hannay, The Clausius–Mossotti equation: an alternative derivation. Eur. J. Phys. **4**, 141–143 (1983)
4. JC Maxwell Garnett, XII Colours in metal glasses and in metallic films. Philos. Trans. R. Soc. A **203**, 385–420 (1904)
5. S.M. Rytov, Electromagnetic properties of a finely stratified medium. Sov. Phys. JETP **2**, 466–475 (1956)
6. V.G. Veselago, The electrodynamics of substances with simultaneously negative values of ε and μ. Sov. Phys. Usp. **10**, 509–514 (1968)
7. D.R. Smith, J.B. Pendry, Homogenization of metamaterials by field averaging (invited paper). J. Opt. Soc. Am. B **23**(3), 391–403 (2006)
8. V.V. Gozhenko, A.K. Amert, K.W Whites, Homogenization of periodic metamaterials by field averaging over unit cell boundaries: use and limitations, New J. Phys. **15**, art. 043030 (2013)
9. J.S. Pérez-Huerta, G.P. Ortiz, B.S. Mendoza, W.L. Mochán, Macroscopic optical response and photonic bands, New J. Phys. **15**, art. 043037 (2013)
10. W. Mochan, R.G. Barrera, Electromagnetic response of systems with spatial fluctuations. I. General formalism. Phys. Rev. B **32**(8), 4984–4988 (1985)
11. W.L. Mochan, G.P. Ortiz, B.S. Mendoz, Efficient homogenization procedure for the calculation of optical properties of 3D nanostructured composites. Opt. Express **18**(21), 22119–22127 (2010)
12. C. Fietz, Y. Urzhumov, G. Shvets, Complex k band diagrams of 3D metamaterial/photonic crystals. Opt. Express **19**(20), 19027–19041 (2011)
13. H. Nikkhah, T. Hall, Metamaterial Lüneburg lens for Fourier optics on-a-chip, SPIE OPTO. Int. Soc. Opt. Photon. (2014). doi:10.1117/12.2040220
14. B. Vasic, G. Isic, R. Gajic, K. Hingerl, Controlling electromagnetic fields with graded photonic crystals in metamaterial regime. Opt. Express **18**(19), 20321–20333 (2010)
15. M. Hasan, R. Guemri, R. Maldonado-Basilio, F. Lucarz, J. de Bougrenet de la Tocnaye, T.J. Hall, Theoretical analysis and modeling of a photonic integrated circuit for frequency 8-tupled and 24-tupled millimeter wave signal generation. Opt. Lett. **39**(24), 6950–6953 (2014)
16. M. Hasan, R. Maldonado-Basilio, T.J. Hall, Comments on X. Yin, A. Wen, Y. Chen, and T. Wang, 'Studies in an optical millimeter-wave generation scheme via two parallel dual-parallel Mach-Zehnder modulators', Journal of Modern Optics, 58(8), 2011, pp. 665-673. J. Mod. Opt. **62**(7), 581–583 (2015)
17. R. Maldonado-Basilio, M. Hasan, H. Nikkhah, S. Abdul-Majid, R. Guemri, F. Lucarz, J.-L. de Bougrenet de la Tocnaye, T.J. Hall, Electro-optic up-conversion mixer amenable to photonic integration, J. Mod. Opt. **62**(17), 1405–1411 (2015)
18. M. Hasan, R. Maldonado-Basilio, T.J. Hall, Dual-function photonic integrated circuit for frequency octo-tupling or single-sideband modulation. Opt. Lett. **40**, 2501–2504 (2015)
19. R. Maldonado-Basilio, M. Hasan, R. Guemri, F. Lucarz, T. J. Hall, Generalized mach-zehnder interferometer architectures for radio frequency translation and multiplication: suppression of unwanted harmonics by design, Opt. Commun. **354**, 122–127 (2015)
20. S. Abdul-Majid, I.I. Hasan, P.J. Bock, T.J. Hall, Design, simulation and fabrication of a 90 degrees SOI optical hybrid based on the self-imaging principle. in Photonics Europe 2010, Conference on Silicon Photonics and Photonic Integrated Circuits II, Brussels, Belgium, 12–16 April, Proc SPIE, 7719, 2010, art. 77190E, 2010